



Alpha-decay properties of nuclei around neutron magic numbers

Ming Li¹ · Chu-Xin Chen² · Lan-Fang Xiao³ · Yi Zhang⁴ · Song Luo¹ · Xiao-Hua Li^{1,5,6,7}

Received: 9 May 2024 / Revised: 14 August 2024 / Accepted: 31 August 2024 / Published online: 20 December 2024

© The Author(s), under exclusive licence to China Science Publishing & Media Ltd. (Science Press), Shanghai Institute of Applied Physics, the Chinese Academy of Sciences, Chinese Nuclear Society 2024

Abstract

By combining experimental α -decay energies and half-lives, the α -particle preformation factor for nuclei around neutron magic numbers N of 126, 152, and 162 were extracted using the two-potential approach. The nuclei around the shell closure were more tightly bound than adjacent nuclei. Additionally, based on the WS4 mass model (Wang et al., Phys. Lett. B **734**, 215 (2014)), we extended the two-potential approach to predict the α -decay half-lives of nuclei around N values of 178 and 184 with Z of 119 and 120. We believe that our findings will serve as guidelines for future experimental studies.

Keywords α decay · Preformation factor · Neutron magic number · Heavy and superheavy nuclei

1 Introduction

The exploration of nuclear structures is a prevalent area in nuclear physics [1–8]. α decay, as the dominant decay mode of heavy and superheavy nuclei, has long been regarded as a reliable pathway for obtaining rich nuclear information

such as the decay energy [9–12], half-life [13–18], shell effect [19], and deformation [20–27]. This decay process was explained by Gamow [28] and Condon and Gurney [29] as a quantum tunneling effect back in 1928. Subsequently, numerous phenomenological models have been proposed to study α decay, such as the density-dependent cluster model [30, 31], two-potential approach (TPA) [16, 32], generalized liquid-drop model [33–35], and unified fission model [36]. These methods suitably reproduce the experimental half-lives and are widely used to further predict the half-lives of unknown nuclei for subsequent experimental studies.

In recent years, with the development of experimental equipment, many studies have been devoted to heavy and superheavy nuclei to extract valuable nuclear structure information from such extreme nuclei [37–41]. Superheavy elements 110–118 have been successfully

This work was supported in part by the National Natural Science Foundation of China (Nos. 12175100 and 11975132), Construct Program of the Key Discipline in Hunan Province, Research Foundation of Education Bureau of Hunan Province, China (Nos. 21B0402, 18A237 and 22A0305), Natural Science Foundation of Hunan Province, China (No. 2018JJ2321), Innovation Group of Nuclear and Particle Physics in USC, Shandong Province Natural Science Foundation, China (No. ZR2022JQ04), Opening Project of Cooperative Innovation Center for Nuclear Fuel Cycle Technology and Equipment, University of South China (No. 2019KFZ10), and Hunan Provincial Innovation Foundation for Postgraduate (No. CX20230962).

✉ Chu-Xin Chen
18073526090@163.com

✉ Song Luo
luosongphysics@126.com

✉ Xiao-Hua Li
lixiaohuaphysics@126.com

¹ School of Nuclear Science and Technology, University of South China, Hengyang 421001, China

² PET-CT Center, Chenzhou First People's Hospital, Chenzhou 423000, China

³ Hengyang Ecological Environment Monitor Center, Hengyang 421001, China

⁴ China Certification and Inspection Group, Hefei 230000, China

⁵ National Exemplary Base for International Science and Technology Collaboration of Nuclear Energy and Nuclear Safety, University of South China, Hengyang 421001, China

⁶ Cooperative Innovation Center for Nuclear Fuel Cycle Technology and Equipment, University of South China, Hengyang 421001, China

⁷ Key Laboratory of Low Dimensional Quantum Structures and Quantum Control, Hunan Normal University, Changsha 410081, China

synthesized using different fusion reactions, advancing toward the superheavy stable island [42–45]. On the other hand, increasing experimental data suggest that nuclei around magic numbers are relatively more stable in heavy and superheavy regions. These include neutron magic numbers, N , of 126, 152, and 162 [46–48]. In fact, the traditional liquid-drop model indicates that superheavy nuclei cannot exist because of their strong Coulomb potentials. In the 1980s, corresponding experiments confirmed that a region of deformed superheavy nuclei exists near proton and neutron numbers of 108 and 162, respectively [49]. Many studies have shown that the shell effect in the deformed regions contributes to maintain the stability of superheavy nuclei [50, 51]. As a magic number is usually a good indicator of the shell structure, the α -decay properties of nuclei should be investigated around neutron magic numbers in the heavy and superheavy regions. First, nuclei around neutrons contain important nuclear structure information. Second, research based on α -decay properties can be extended to predict the half-lives of unknown nuclei to provide reasonable references for subsequent experiments. In addition, relevant studies have suggested that N values of 178 and 184 are candidate neutron magic numbers in superheavy regions [15, 35, 52]. Similarly, the corresponding decay properties of related nuclei should be unveiled.

In α decay, the α -particle preformation factor represents the relative probability of four nucleons forming an α cluster on the surface or inside the parent nucleus [53, 54]. As this factor largely depends on the structures and states of the parent and daughter nuclei, it is often regarded as a useful probe for studying nuclear structures [55–58]. In a recent study, by combining the experimental decay energy and half-life, we systematically extracted the α -particle preformation factor of heavy and superheavy nuclei using the TPA. The TPA [16, 32, 48] is a phenomenological model that can describe α decay, and it has been extended to describe proton radioactivity [59], with the calculated half-lives suitably agreeing with experimental data. In the present study, by combining experimental half-life and decay energy data, we further extended the TPA to extract the α -particle preformation factor of nuclei around neutron magic numbers, N , of 126, 152, and 162. Useful nuclear structure information was obtained from the relevant α -decay properties. In addition, we extended the model to predict the α -decay half-lives of the nuclei around N of 178 and 184 with Z of 119 and 120. Our findings may provide useful guidelines for future synthetic experiments.

The remainder of this paper is organized as follows. Section 2 details the TPA framework and α -particle preformation factor. The results and discussion are presented in Sect. 3. Finally, a summary of the study and findings is presented in Sect. 4.

2 Theoretical framework

2.1 TPA

In the TPA framework, the α -decay half-life, $T_{1/2}$, is given by

$$T_{1/2} = \frac{\ln 2}{\lambda}, \tag{1}$$

where λ is the decay constant. Under the TPA framework, the decay constant is typically related to three parts: normalized factor F , penetration probability P , and α -particle preformation factor P_α . In the TPA, the decay constant can be described as

$$\lambda = \frac{\hbar P_\alpha F P}{4\mu}, \tag{2}$$

where \hbar denotes Planck’s constant. F is the normalized factor of the bound-state wave function, which is an important physical quantity related to the collision frequency and satisfies the following condition:

$$F \int_{r_1}^{r_2} \frac{1}{2k(r)} dr = 1, \tag{3}$$

where r is the distance between the centers of mass of the daughter nucleus and preformed α particle, while $k(r)$ denotes the wave number expressed as

$$k(r) = \sqrt{\frac{2\mu}{\hbar^2} |Q_\alpha - V(r)|}, \tag{4}$$

with Q_α and $V(r)$ denoting the α -decay energy and total interaction potential, respectively. Penetration probability P can be calculated using the classical Wentzel–Kramers–Brillouin approximation:

$$P = \exp \left[-2 \int_{r_2}^{r_3} k(r) dr \right], \tag{5}$$

where r_1 , r_2 , and r_3 are classical turning points that satisfy $V(r_1) = V(r_2) = V(r_3) = Q_\alpha$.

Table 1 Parameter values for estimating α -particle preformation factors in Eq. (12)

Nuclei	a	b	c	d	h
Even-Even nuclei				0	0
Odd- A nuclei	0.035	−1.406	7.070	−0.054	−0.4687
Odd-Odd nuclei				−0.054	−0.9374

Parameters a , b , and c share the same numerical results for different nuclei

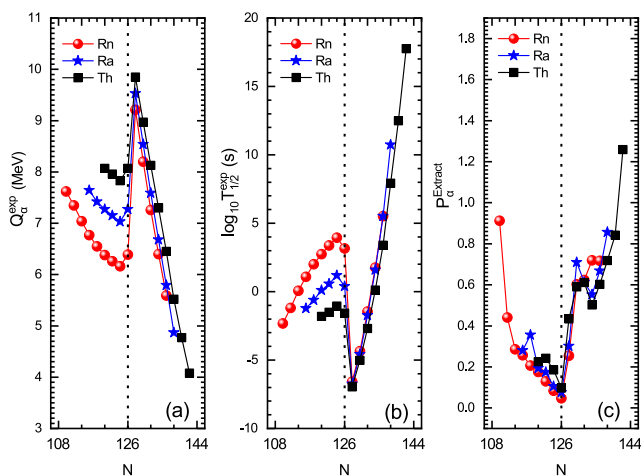


Fig. 1 (Color online) α -decay properties of nuclei around neutron magic number N of 126. **a** Variations in experimental α -decay energy according to neutron number of parent nuclei. Variations in **b** experimental half-lives and **c** extracted preformation factors according to neutron number of parent nuclei. The red circles, blue stars, and black squares represent the results of Rn, Ra, and Th isotopes, respectively

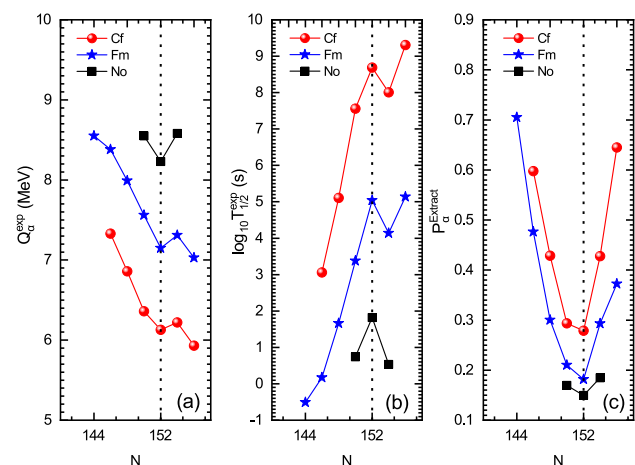


Fig. 2 (Color online) Similar comparison to that shown in Fig. 1 for α -decay properties of nuclei around neutron magic number N of 152. The red circles, blue stars, and black squares represent the results of Cf, Fm, and No isotopes, respectively

The total interaction potential, $V(r)$, can be divided into three components: nuclear potential $V_N(r)$, Coulomb potential $V_C(r)$, and centrifugal potential $V_l(r)$. In addition, we mainly focus on the nuclear structure information derived from even–even nuclei to avoid any obvious odd–even staggering effects on the binding energy [60] or preformation factors [48, 50] while emphasizing shell effects. According to the conservation laws of spin parity, centrifugal potential $V_l(r)$ of even–even nuclei is treated

as zero. In addition, we choose the following hyperbolic cosine parameterized form for the nuclear potential:

$$V_N(r) = -V_0 \frac{1 + \cosh(R/a)}{\cosh(r/a) + \cosh(R/a)}, \quad (6)$$

where V_0 and a are the depth and diffuseness parameters of the nuclear potential, respectively. Additional details can be found in [16, 32, 48]. Assuming a uniformly charged sphere, Coulomb potential $V_C(r)$ can be expressed as

$$V_C(r) = \begin{cases} \frac{Z_d Z_\alpha e^2}{2R} \left[3 - \frac{r^2}{R^2} \right], & r \leq R, \\ \frac{Z_d Z_\alpha e^2}{r}, & r > R, \end{cases} \quad (7)$$

where Z_d and Z_α are the charge numbers of the daughter nucleus and α particle, respectively. Referring to the liquid-drop model, radius R [61] can be expressed as

$$R = 1.28A^{1/3} - 0.76 + 0.8A^{-1/3}. \quad (8)$$

2.2 α -particle preformation factor

We obtain the α -particle preformation factor, $P_\alpha^{\text{Extract}}$, from the ratios between the theoretical α -decay half-life calculated by TPA and corresponding experimental value. Considering Eqs. (1) and (2), the experimental decay constant, λ_{exp} , can be calculated as

$$\lambda_{\text{exp}} = \frac{\ln 2}{T_{1/2}^{\text{exp}}} = \frac{\hbar P_\alpha^{\text{Extract}} F P}{4\mu}. \quad (9)$$

Assuming preformation factor $P_\alpha = 1.0$, theoretical decay constant λ_{cal} can be expressed as

$$\lambda_{\text{cal}} = \frac{\ln 2}{T_{1/2}^{\text{cal}}} = \frac{\hbar P_\alpha F P}{4\mu}. \quad (10)$$

Combining Eqs. (9) and (10), the α -particle preformation factor can be extracted from the ratio between the theoretical α -decay half-life and corresponding experimental value as follows:

$$P_\alpha^{\text{Extract}} = \frac{\lambda_{\text{exp}}}{\lambda_{\text{cal}}} = \frac{T_{1/2}^{\text{cal}}}{T_{1/2}^{\text{exp}}}. \quad (11)$$

2.3 Phenomenological formula for estimating α -particle preformation factor

We also predict the α -decay half-lives for unknown nuclei around the neutron magic numbers, which are important

Table 2 Extracted α -particle preformation factors and calculated half-lives for nuclei around neutron magic number N of 126

α transition	N	Q_{α}^{exp} (MeV)	$P_{\alpha}^{\text{Extract}}$	$\log_{10} T_{1/2}^{\text{exp}}$ (s)	$\log_{10} T_{1/2}^{\text{cal 1}}$ (s)
$Z = 86$					
$^{196}\text{Rn} \rightarrow ^{192}\text{Po} + \alpha$	110	7.62	0.9127	-2.33	-2.37
$^{198}\text{Rn} \rightarrow ^{194}\text{Po} + \alpha$	112	7.35	0.4408	-1.18	-1.54
$^{200}\text{Rn} \rightarrow ^{196}\text{Po} + \alpha$	114	7.04	0.2853	0.07	-0.47
$^{202}\text{Rn} \rightarrow ^{198}\text{Po} + \alpha$	116	6.77	0.2562	1.09	0.50
$^{204}\text{Rn} \rightarrow ^{200}\text{Po} + \alpha$	118	6.55	0.2067	2.01	1.33
$^{206}\text{Rn} \rightarrow ^{202}\text{Po} + \alpha$	120	6.38	0.1751	2.74	1.98
$^{208}\text{Rn} \rightarrow ^{204}\text{Po} + \alpha$	122	6.26	0.1295	3.37	2.48
$^{210}\text{Rn} \rightarrow ^{206}\text{Po} + \alpha$	124	6.16	0.0839	3.95	2.87
$^{212}\text{Rn} \rightarrow ^{208}\text{Po} + \alpha$	126	6.39	0.0471	3.16	1.83
$^{214}\text{Rn} \rightarrow ^{210}\text{Po} + \alpha$	128	9.21	0.2543	-6.57	-7.16
$^{216}\text{Rn} \rightarrow ^{212}\text{Po} + \alpha$	130	8.20	0.6021	-4.35	-4.57
$^{218}\text{Rn} \rightarrow ^{214}\text{Po} + \alpha$	132	7.26	0.6232	-1.46	-1.67
$^{220}\text{Rn} \rightarrow ^{216}\text{Po} + \alpha$	134	6.40	0.7197	1.75	1.61
$^{222}\text{Rn} \rightarrow ^{218}\text{Po} + \alpha$	136	5.59	0.7176	5.52	5.38
$Z = 88$					
$^{204}\text{Ra} \rightarrow ^{200}\text{Rn} + \alpha$	116	7.64	0.2803	-1.22	-1.77
$^{206}\text{Ra} \rightarrow ^{202}\text{Rn} + \alpha$	118	7.42	0.3563	-0.62	-1.07
$^{208}\text{Ra} \rightarrow ^{204}\text{Rn} + \alpha$	120	7.27	0.1937	0.10	-0.61
$^{210}\text{Ra} \rightarrow ^{206}\text{Rn} + \alpha$	122	7.15	0.1739	0.57	-0.19
$^{212}\text{Ra} \rightarrow ^{208}\text{Rn} + \alpha$	124	7.03	0.1049	1.18	0.20
$^{214}\text{Ra} \rightarrow ^{210}\text{Rn} + \alpha$	126	7.27	0.0746	0.39	-0.74
$^{216}\text{Ra} \rightarrow ^{212}\text{Rn} + \alpha$	128	9.53	0.3014	-6.74	-7.26
$^{218}\text{Ra} \rightarrow ^{214}\text{Rn} + \alpha$	130	8.54	0.7092	-4.59	-4.74
$^{220}\text{Ra} \rightarrow ^{216}\text{Rn} + \alpha$	132	7.59	0.6122	-1.74	-1.95
$^{222}\text{Ra} \rightarrow ^{218}\text{Rn} + \alpha$	134	6.68	0.5521	1.59	1.33
$^{224}\text{Ra} \rightarrow ^{220}\text{Rn} + \alpha$	136	5.79	0.6687	5.52	5.35
$^{226}\text{Ra} \rightarrow ^{222}\text{Rn} + \alpha$	138	4.87	0.8564	10.73	10.66
$Z = 90$					
$^{210}\text{Th} \rightarrow ^{206}\text{Ra} + \alpha$	120	8.07	0.2250	-1.80	-2.45
$^{212}\text{Th} \rightarrow ^{208}\text{Ra} + \alpha$	122	7.96	0.2425	-1.50	-2.12
$^{214}\text{Th} \rightarrow ^{210}\text{Ra} + \alpha$	124	7.83	0.1853	-1.06	-1.79
$^{216}\text{Th} \rightarrow ^{212}\text{Ra} + \alpha$	126	8.07	0.0968	-1.57	-2.58
$^{218}\text{Th} \rightarrow ^{214}\text{Ra} + \alpha$	128	9.85	0.4338	-6.96	-7.32
$^{220}\text{Th} \rightarrow ^{216}\text{Ra} + \alpha$	130	8.97	0.5902	-5.01	-5.24
$^{222}\text{Th} \rightarrow ^{218}\text{Ra} + \alpha$	132	8.13	0.6108	-2.69	-2.90
$^{224}\text{Th} \rightarrow ^{220}\text{Ra} + \alpha$	134	7.30	0.5017	0.12	-0.18
$^{226}\text{Th} \rightarrow ^{222}\text{Ra} + \alpha$	136	6.45	0.6021	3.39	3.17
$^{228}\text{Th} \rightarrow ^{224}\text{Ra} + \alpha$	138	5.52	0.7179	7.93	7.79
$^{230}\text{Th} \rightarrow ^{226}\text{Ra} + \alpha$	140	4.77	0.8421	12.49	12.42
$^{232}\text{Th} \rightarrow ^{230}\text{Ra} + \alpha$	142	4.08	1.2594	17.76	17.86

The experimental α -decay energies and half-lives were retrieved from [67–71]. The decay energies and half-lives were measured in mega-electron volts and seconds, respectively

indicators. However, such prediction does not allow to evaluate the α -particle preformation factor for unknown nuclei. In [48], we proposed a local phenomenological formula to

estimate the α -particle preformation factor for heavy and superheavy nuclei. The estimated preformation factor by the analytical expression is denoted as P_{α}^{Eq} . This analytical

expression can describe the α -particle preformation factor extracted from experimental data and facilitate accurate half-life calculation. The analytical expression is given by

$$\log_{10} P_{\alpha}^{\text{Eq}} = aZQ_{\alpha}^{-1/2} + bA^{1/3} + c + dl + h, \quad (12)$$

where a , b , c , d , and h are related parameters with values obtained by fitting the preformation factors extracted from experimental data. The detailed values for different nuclei are listed in Table 1. Z , A , and Q_{α} represent the proton number, mass number of the parent nucleus, and α -decay energy, respectively, and l represents the angular momentum removed by the emitted α particles.

3 Results and discussion

An N value of 126 is a classical neutron magic number [46]. Thus, the α -decay properties of nuclei around N of 126 can be considered as a reference for larger neutron magic numbers in the heavy and superheavy regions. Using Eq. (11), the α -particle preformation factors for Rn, Ra, and Th isotopes were obtained as listed in Table 2. The first three columns indicate the α transition, neutron number of the parent nucleus, and experimental decay energy. The fourth column indicates the prediction factors extracted from experimental data, denoted by $P_{\alpha}^{\text{Extract}}$. The last two columns denote the logarithmic form of the experimental α -decay half-lives and those calculated using $P_{\alpha} = 1.0$. To visualize the nuclear

structure information reflected by the corresponding decay properties, the variations in the experimental α -decay energies (panel (a)), half-lives (panel (b)), and extracted preformation factors (panel (c)) according to neutron number N are shown for Rn, Ra, and Th isotopes in Fig. 1. Panels (a) and (b) show that the decay energies for each isotope chain generally decrease with increasing neutron number. A clear reversal occurs at N of 126 with a rapid increase until N of 128. In addition, the half-life of each isotope chain generally increases with increasing neutron number. However, a substantial decline begins at N of 126 until N of 128. At N of 126 in the classic neutron shell closure, a sharp peak in the decay energy and minimum in the half-life at N of 128 indicate the “magicity” of the daughter nuclei for N of 126. These results also indicate that the nuclei are more stable with closed shells. Similar results were reported in [62] and [63]. In panel (c), the preformation factors show the lowest values for Rn, Ra, and Th isotopes for N of 126. This indicates the difficulty of forming an α particle on the surface or inside the parent nucleus when the nucleons occupy the shell closure [47, 48, 55].

Overall, we evaluated the α -decay properties of nuclei around N of 126, finding that the variations in α -decay energies and half-lives exhibited an obvious change when the nuclei were near the shell closure. The preformation factors suggested that the shell effect contributed to maintain nuclear stability. These features provide guidelines for future research. Below, we analyze the α -decay properties of nuclei around N values of 152 and 162.

Table 3 Results as those presented in Table 2 for nuclei around neutron magic number N of 152

α transition	N	Q_{α}^{exp} (MeV)	$P_{\alpha}^{\text{Extract}}$	P_{α}^{Eq}	$\log_{10} T_{1/2}^{\text{exp}}$ (s)	$\log_{10} T_{1/2}^{\text{call}}$ (s)	$\log_{10} T_{1/2}^{\text{cal2}}$ (s)
$Z = 98$							
$^{244}\text{Cf} \rightarrow ^{240}\text{Cm} + \alpha$	146	7.33	0.5978	0.3654	3.06	2.84	3.27
$^{246}\text{Cf} \rightarrow ^{242}\text{Cm} + \alpha$	148	6.86	0.4288	0.3820	5.11	4.74	5.16
$^{248}\text{Cf} \rightarrow ^{244}\text{Cm} + \alpha$	150	6.36	0.2936	0.4067	7.56	7.03	7.42
$^{250}\text{Cf} \rightarrow ^{246}\text{Cm} + \alpha$	152	6.13	0.2790	0.4085	8.69	8.14	8.52
$^{252}\text{Cf} \rightarrow ^{248}\text{Cm} + \alpha$	154	6.22	0.4276	0.3780	8.01	7.64	8.06
$^{254}\text{Cf} \rightarrow ^{250}\text{Cm} + \alpha$	156	5.93	0.6448	0.3869	9.31	9.12	9.53
$Z = 100$							
$^{244}\text{Fm} \rightarrow ^{240}\text{Cf} + \alpha$	144	8.55	0.7051	0.3105	-0.51	-0.66	-0.15
$^{246}\text{Fm} \rightarrow ^{242}\text{Cf} + \alpha$	146	8.3	0.4765	0.3023	0.17	-0.15	0.37
$^{248}\text{Fm} \rightarrow ^{244}\text{Cf} + \alpha$	148	7.99	0.3002	0.3063	1.66	1.14	1.65
$^{250}\text{Fm} \rightarrow ^{246}\text{Cf} + \alpha$	150	7.56	0.2100	0.3144	3.38	2.70	3.20
$^{252}\text{Fm} \rightarrow ^{248}\text{Cf} + \alpha$	152	7.15	0.1814	0.3238	5.04	4.30	4.79
$^{254}\text{Fm} \rightarrow ^{250}\text{Cf} + \alpha$	154	7.31	0.2929	0.2967	4.14	3.61	4.13
$^{256}\text{Fm} \rightarrow ^{252}\text{Cf} + \alpha$	156	7.03	0.3724	0.2987	5.14	4.71	5.24
$Z = 102$							
$^{252}\text{No} \rightarrow ^{248}\text{Fm} + \alpha$	150	8.55	0.1696	0.2638	0.74	-0.03	0.55
$^{254}\text{No} \rightarrow ^{250}\text{Fm} + \alpha$	152	8.23	0.1496	0.2640	1.82	1.00	1.57
$^{256}\text{No} \rightarrow ^{252}\text{Fm} + \alpha$	154	8.58	0.1848	0.2357	0.53	-0.20	0.42

Table 4 Results as those presented in Table 3 for nuclei around neutron magic number N of 162

α transition	N	Q_α^{exp} (MeV)	$P_\alpha^{\text{Extract}}$	P_α^{Eq}	$\log_{10} T_{1/2}^{\text{exp}}$ (s)	$\log_{10} T_{1/2}^{\text{cal 1}}$ (s)	$\log_{10} T_{1/2}^{\text{cal 2}}$ (s)
$Z = 106$							
$^{260}\text{Sg} \rightarrow ^{256}\text{Rf} + \alpha$	154	9.90	0.2378	0.1932	-2.04	-2.66	-1.95
$Z = 108$							
$^{266}\text{Hs} \rightarrow ^{262}\text{Sg} + \alpha$	158	10.35	0.1450	0.1634	-2.41	-3.25	-2.46
$^{268}\text{Hs} \rightarrow ^{264}\text{Sg} + \alpha$	160	9.77	0.0452	0.1680	-0.39	-1.74	-0.96
$^{270}\text{Hs} \rightarrow ^{266}\text{Sg} + \alpha$	162	9.07	0.1326	0.1775	1.18	0.30	1.05
$Z = 110$							
$^{270}\text{Ds} \rightarrow ^{266}\text{Hs} + \alpha$	160	11.12	0.0154	0.1404	-2.70	-4.51	-3.66
$^{282}\text{Ds} \rightarrow ^{278}\text{Hs} + \alpha$	172	9.15	0.0565	0.1363	1.82	0.57	1.44

In [12, 15, 48, 51], we showed that the deformed shell effect around N of 152 was mainly concentrated in the region near a Z value of 100. Combined with the latest experimental data, we focused on the Cf–No (Z values from 98 to 102) isotope chains to study the α -decay properties because available experimental data were insufficient to support analyze other isotope chains. The α -particle preformation factors for Cf, Fm, and No isotopes were obtained as listed in Table 3. The first three columns indicate the α transition, neutron number of the parent nucleus, and experimental decay energy. The fourth and fifth columns indicate the extracted preformation factors from the relevant experimental data and values estimated using Eq. (12), denoted as $P_\alpha^{\text{Extract}}$ and P_α^{Eq} , respectively. The sixth

column shows the experimental half-lives. The last two columns indicate the calculated half-lives in logarithmic form with the corresponding preformation factors derived at $P_0 = 1.0$ from Eq. (12), denoted as $\log_{10} T_{1/2}^{\text{cal 1}}$ and $\log_{10} T_{1/2}^{\text{cal 2}}$, respectively. The estimation of the preformation factors and predictions of the half-lives are discussed below. The variations in the α -decay energies (panel (a)), half-lives (panel (b)), and preformation factors (panel (c)) according to neutron number N are shown for Cf, Fm, and No isotopes in Fig. 2. The variations in the decay energies and half-lives differ for N of 152. Similarly, the nuclei near neutron magic number N of 152 have longer half-lives than the corresponding adjacent nuclei. Microscopically, the preformation factors revealed useful nuclear structure information, that is, smaller prediction factors indicated a higher difficulty of forming an α particle inside the nucleus. Under these conditions, the relevant decay processes were inhibited. These results provide valuable guidelines for experimental designs in this region.

Table 5 Predicted preformation factors and α -decay half-lives for nuclei around neutron magic number N of 126 by inputting Q_α values extracted from WS4 mass model [64]. The decay energies and half-lives were measured in mega-electron volts and seconds, respectively

α transition	N	Q_α^{WS4} (MeV)	P_α^{Eq}	$\log_{10} T_{1/2}^{\text{cal}}$ (s)
$Z = 106$				
$^{262}\text{Sg} \rightarrow ^{258}\text{Rf} + \alpha$	156	9.65	0.1851	-1.28
$^{264}\text{Sg} \rightarrow ^{260}\text{Rf} + \alpha$	158	9.05	0.1922	0.43
$^{266}\text{Sg} \rightarrow ^{262}\text{Rf} + \alpha$	160	8.44	0.2017	2.34
$^{268}\text{Sg} \rightarrow ^{264}\text{Rf} + \alpha$	162	7.98	0.2082	3.98
$^{270}\text{Sg} \rightarrow ^{266}\text{Rf} + \alpha$	164	8.56	0.1781	1.92
$^{272}\text{Sg} \rightarrow ^{268}\text{Rf} + \alpha$	166	8.42	0.1733	2.40
$Z = 108$				
$^{272}\text{Hs} \rightarrow ^{268}\text{Sg} + \alpha$	164	9.53	0.1530	-0.31
$^{274}\text{Hs} \rightarrow ^{270}\text{Sg} + \alpha$	166	9.50	0.1460	-0.28
$^{276}\text{Hs} \rightarrow ^{272}\text{Sg} + \alpha$	168	9.05	0.1487	1.07
$Z = 110$				
$^{272}\text{Ds} \rightarrow ^{266}\text{Hs} + \alpha$	162	10.38	0.1430	-1.89
$^{274}\text{Ds} \rightarrow ^{266}\text{Hs} + \alpha$	164	10.87	0.1276	-3.09
$^{276}\text{Ds} \rightarrow ^{266}\text{Hs} + \alpha$	166	10.88	0.1211	-3.13
$^{278}\text{Ds} \rightarrow ^{266}\text{Hs} + \alpha$	168	10.25	0.1248	-1.64
$^{280}\text{Ds} \rightarrow ^{266}\text{Hs} + \alpha$	170	9.43	0.1335	0.62

The α -decay properties of nuclei around neutron magic number N of 162 appeared to be more complex than those for other numbers. First, $^{270}\text{Hs}_{162}$ have been experimentally demonstrated to be a deformed double magic nucleus [49]. Although the shell effect around this region may also originate from the proton shell, insufficient experimental data impede further investigation of the shell effect in this region. Available experimental data for Hs, Sg, and Ds isotopes are listed in Table 4, which is organized as Table 3. No complete isotopes with $N > 162$ appeared, and the data distribution was very scattered. Under these conditions, it was difficult to determine the relevant nuclear structure information. Instead, we attempted to find a bridge for the scattered nuclei and predict the decay energies and half-lives of these unknown nuclei. In turn, these predictions allowed us to investigate the possible nuclear structural features in the superheavy region and might be useful for experiments in the future work.

In [52], the α -decay energies extracted from the WS4 mass table [64] were the most accurate for reproducing

Table 6 Calculated $\log_{10} T_{1/2}$ values for isotopes with Z values of 119 and 120 by inputting Q_α values extracted from WS4 mass model [64]

Nuclei	N	Q_α^{WS4} (MeV)	P_α^{Eq}	$\log_{10} T_{1/2}$ (s)
$^{290}\text{119}$	171	13.07	0.0095	-4.18
$^{291}\text{119}$	172	13.05	0.0274	-4.64
$^{292}\text{119}$	173	12.90	0.0092	-3.88
$^{293}\text{119}$	174	12.72	0.0270	-4.01
$^{294}\text{119}$	175	12.73	0.0089	-3.57
$^{295}\text{119}$	176	12.76	0.0256	-4.11
$^{296}\text{119}$	177	12.48	0.0087	-3.08
$^{297}\text{119}$	178	12.42	0.0253	-3.40
$^{298}\text{119}$	179	12.71	0.0081	-3.57
$^{299}\text{119}$	180	12.76	0.0232	-4.13
$^{300}\text{119}$	181	12.57	0.0079	-3.30
$^{301}\text{119}$	182	12.43	0.0229	-3.49
$^{302}\text{119}$	183	12.43	0.0076	-3.03
$^{303}\text{119}$	184	12.42	0.0219	-3.46
$^{304}\text{119}$	185	12.93	0.0069	-4.05
$^{305}\text{119}$	186	13.42	0.0188	-5.39
$^{306}\text{119}$	187	13.20	0.0064	-4.56
$^{307}\text{119}$	188	12.78	0.0191	-4.24
$^{308}\text{119}$	189	12.06	0.0069	-2.30
$^{309}\text{119}$	190	11.37	0.0214	-1.22
$^{291}\text{120}$	171	13.51	0.0267	-5.20
$^{292}\text{120}$	172	13.47	0.0089	-4.67
$^{293}\text{120}$	173	13.40	0.0257	-5.03
$^{294}\text{120}$	174	13.24	0.0087	-4.25
$^{295}\text{120}$	175	13.27	0.0248	-4.79
$^{296}\text{120}$	176	13.34	0.0082	-4.47
$^{297}\text{120}$	177	13.14	0.0239	-4.57
$^{298}\text{120}$	178	13.01	0.0081	-3.87
$^{299}\text{120}$	179	13.26	0.0225	-4.80
$^{300}\text{120}$	180	13.32	0.0074	-4.46
$^{301}\text{120}$	181	13.06	0.0219	-4.44
$^{302}\text{120}$	182	12.89	0.0074	-3.66
$^{303}\text{120}$	183	12.81	0.0214	-3.98
$^{304}\text{120}$	184	12.76	0.0072	-3.41
$^{305}\text{120}$	185	13.28	0.0195	-4.89
$^{306}\text{120}$	186	13.79	0.0062	-5.36
$^{307}\text{120}$	187	13.52	0.0181	-5.36
$^{308}\text{120}$	188	12.97	0.0064	-3.86
$^{309}\text{120}$	189	12.16	0.0200	-2.69
$^{310}\text{120}$	190	11.50	0.0072	-0.75

The decay energies and half-lives were measured in mega-electron volts and seconds, respectively

experimental data for superheavy nuclei. The WS4 mass model has been used to predict the α -decay energies of incomplete isotopes. In addition, the α -particle preformation factors should be evaluated for unknown nuclei before predicting their relevant half-lives. In a previous study, we

devised a local phenomenological formula, Eq. (12), to estimate α -particle preformation factors for heavy and superheavy nuclei. Tables 3 and 4 show that the preformation factors evaluated using Eq. (12) (P_α^{Eq}) suitably agreed with the extracted ones ($P_\alpha^{\text{Extract}}$) and that the calculated half-lives ($\log_{10} T_{1/2}^{\text{cal}}$) were consistent with the experimental data ($\log_{10} T_{1/2}^{\text{exp}}$). Accordingly, we extended the TPA to predict the half-lives of unknown nuclei around neutron magic number N of 162. The predicted results are listed in Table 5. The first two columns indicate the α transition and neutron number of the parent nucleus. The third column indicates the predicted α -decay energies extracted from the WS4 mass model. The last two columns indicate the predicted preformation factors and half-lives of the nuclei around N of 162. To clearly show the decay in this region, the variations in the corresponding α -decay energies (panel (a)) and half-lives (panel (b)) according to neutron number N are shown for Sg, Hs, and Ds isotopes in Fig. 3. The red and black symbols represent the experimental data and predicted results, respectively. The variations in the decay energies and half-lives differed for N of 162, although most of the results were derived from the predicted values. Combined with the α -decay properties of the nuclei around N values of 126 and 152, some nuclei around neutron number N of 162 should showed longer half-lives for synthesis or experimental detection. These predictions may provide useful information for future work.

New elements with Z values of 119 and 120 have been experimentally investigated in recent years. Relevant studies have suggested that N of 178 is a neutron magic number, in addition to the well-known neutron magic number, N , of 184 [15, 35, 52]. Therefore, we also predicted the α -decay half-lives of nuclei with Z values of 119 and

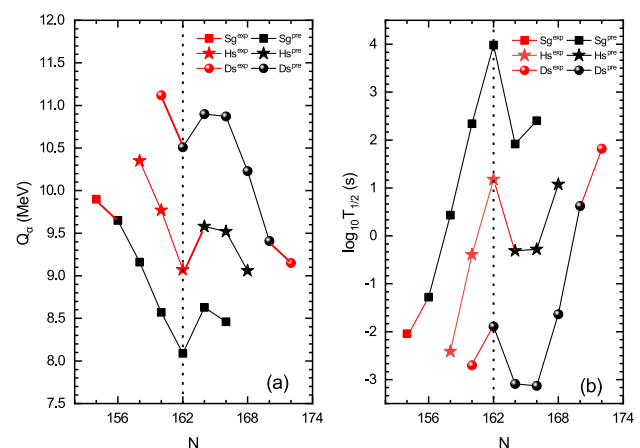


Fig. 3 (color online) Similar comparison to that shown in Fig. 1 for α -decay properties of nuclei around neutron magic number N of 162. The red and black symbols indicate experimental data and predicted results, respectively

120 around N of 178 and 184, respectively [17, 18, 65, 66]. Using the α -decay energies extracted from the WS4 mass model [64] and preformation factors estimated using Eq. (12), the TPA was applied to predict the half-lives of the unknown nuclei. The relevant decay processes were assumed to be transitions from ground-to-ground state. The predicted results are listed in Table 6, which is organized as Table 5. These predictions may provide valuable guidelines for future experiments.

4 Summary

We systematically investigated the α -decay properties of nuclei around neutron magic numbers N of 126, 152, and 162. By combining the experimental α -decay energies and half-lives, the α -particle preformation factors for the nuclei around these magic numbers were obtained using the TPA. Useful nuclear structure information was also obtained. More importantly, the TPA was extended to predict the α -decay half-lives of the nuclei around N values of 178 and 184 with Z values of 119 and 120. Our findings will likely provide guidelines for further synthesis experiments.

Author Contributions All authors contributed to the study conception and design. Material preparation, data collection, and analysis were performed by ML, SL, CXC, XHL, LFX, and YZ. The first draft of the manuscript was written by ML, and all authors commented on previous versions of the manuscript. All authors read and approved the final manuscript.

Data availability statement The data that support the findings of this study are openly available in Science Data Bank at <https://cstr.cn/31253.11.sciencedb.j00186.00321> and <https://www.doi.org/10.57760/sciencedb.j00186.00321>.

Declarations

Conflict of interest The authors declare that they have no conflict of interest.

References

1. B. Blank, M.J.G. Borge, Nuclear structure at the proton drip line: advances with nuclear decay studies. *Prog. Part. Nucl. Phys.* **60**, 403 (2008). <https://doi.org/10.1016/j.pnpnp.2007.12.001>
2. H.F. Zhang, Y.J. Wang, J.M. Dong et al., Concise methods for proton radioactivity. *J. Phys. G Nucl. Part. Phys.* **37**, 085107 (2010). <https://doi.org/10.1088/0954-3899/37/8/085107>
3. D.S. Delion, R.J. Liotta, R. Wyss, Systematics of proton emission. *Phys. Rev. Lett.* **96**, 072501 (2006). <https://doi.org/10.1103/PhysRevLett.96.072501>
4. J.P. Cui, Y.H. Gao, Y.Z. Wang et al., Two-proton radioactivity within a generalized liquid drop model. *Phys. Rev. C* **101**, 014301 (2020). <https://doi.org/10.1103/PhysRevC.101.014301>
5. H. Jiang, G.J. Fu, Y.M. Zhao et al., Nuclear mass relations based on systematics of proton-neutron interactions. *Phys. Rev. C* **82**, 054317 (2010). <https://doi.org/10.1103/PhysRevC.82.054317>
6. Y.Z. Wang, F.Z. Xing, Y. Xiao et al., An improved semi-empirical relationship for cluster radioactivity. *Chin. Phys. C* **45**, 044111 (2021). <https://doi.org/10.1088/1674-1137/abe112>
7. D.M. Zhang, L.J. Qi, D.X. Zhu et al., Systematic study on the proton radioactivity of spherical proton emitters. *Nucl. Sci. Tech.* **34**, 55 (2023). <https://doi.org/10.1007/s41365-023-01201-7>
8. Y.Y. Xu, X.Y. Hu, D.X. Zhu et al., Systematic study of proton radioactivity half lives. *Nucl. Sci. Tech.* **34**, 30 (2023). <https://doi.org/10.1007/s41365-023-01178-3>
9. J.M. Dong, W. Zuo, W. Scheid, Correlation between α -decay energies of superheavy nuclei involving the effects of symmetry energy. *Phys. Rev. Lett.* **107**, 012501 (2011). <https://doi.org/10.1103/PhysRevLett.107.012501>
10. J.M. Dong, W. Zuo, J.Z. Gu et al., α -decay half-lives and Q_α values of superheavy nuclei. *Phys. Rev. C* **81**, 064309 (2010). <https://doi.org/10.1103/PhysRevC.81.064309>
11. T.K. Dong, Z. Ren, α -decay energy formula for superheavy nuclei based on the liquid-drop model. *Phys. Rev. C* **82**, 034320 (2010). <https://doi.org/10.1103/PhysRevC.82.034320>
12. S. Luo, X. Pan, J.J. Dong et al., An improved α -decay energy formula for heavy and superheavy nuclei. *Commun. Theor. Phys.* **75**, 025301 (2023). <https://doi.org/10.1088/1572-9494/acaaf6>
13. Y.T. Zou, X. Pan, H.M. Liu et al., Systematic studies on α decay half-lives of neptunium isotopes. *Phys. Scr.* **96**, 075301 (2021). <https://doi.org/10.1088/1402-4896/abf795>
14. Y.Y. Xu, D.X. Zhu, X. Chen et al., A unified formula for α decay half-lives. *Eur. Phys. J. A* **58**, 163 (2022). <https://doi.org/10.1140/epja/s10050-022-00812-9>
15. S. Luo, Y.Y. Xu, D.X. Zhu et al., Improved Geiger-Nuttall law for α -decay half-lives of heavy and superheavy nuclei. *Eur. Phys. J. A* **58**, 244 (2022). <https://doi.org/10.1140/epja/s10050-022-00898-1>
16. X.D. Sun, P. Guo, X.H. Li, Systematic study of favored α -decay half-lives of closed shell odd- A and doubly-odd nuclei related to ground and isomeric states. *Phys. Rev. C* **94**, 024338 (2016). <https://doi.org/10.1103/PhysRevC.94.024338>
17. J.P. Cui, Y.H. Gao, Y.Z. Wang et al., Improved effective liquid drop model for α -decay half-lives. *Nucl. Phys. A* **1017**, 122341 (2022). <https://doi.org/10.1016/j.nuclphysa.2021.122341>
18. S. Zhang, Y.L. Zhang, J.P. Cui et al., Improved semi-empirical relationship for α -decay half-lives. *Phys. Rev. C* **95**, 014311 (2017). <https://doi.org/10.1103/PhysRevC.95.014311>
19. P. Arthuis, C. Barbieri, M. Vorabbi et al., Ab initio computation of charge densities for Sn and Xe isotopes. *Phys. Rev. Lett.* **125**, 182501 (2020). <https://doi.org/10.1103/PhysRevLett.125.182501>
20. M.R. Pahlavani, S.A. Alavi, N. Tahanipour, Effect of nuclear deformation on the potential barrier and alpha-decay half-lives of superheavy nuclei. *Mod. Phys. Lett. A* **28**, 1350065 (2013). <https://doi.org/10.1142/S021773231350065X>
21. Y. Su, Z.Y. Li, L.L. Liu et al., Sensitivity impacts owing to the variations in the type of zero-range pairing forces on the fission properties using the density functional theory. *Nucl. Sci. Tech.* **35**, 62 (2024). <https://doi.org/10.1007/s41365-024-01422-4>
22. X. Guan, J.H. Zheng, M.Y. Zheng, Pairing effects on the fragment mass distribution of Th, U, Pu, and Cm isotopes. *Nucl. Sci. Tech.* **34**, 173 (2023). <https://doi.org/10.1007/s41365-023-01316-x>
23. Q.F. Song, L. Zhu, H. Guo et al., Verification of neutron-induced fission product yields evaluated by a tensor decomposition model in transport-burnup simulations. *Nucl. Sci. Tech.* **34**, 32 (2023). <https://doi.org/10.1007/s41365-023-01176-5>

24. B.S. Cai, C.X. Yuan, Random forest-based prediction of decay modes and half-lives of superheavy nuclei. *Nucl. Sci. Tech.* **34**, 204 (2023). <https://doi.org/10.1007/s41365-023-01354-5>
25. V.Y. Denisov, H. Ikezoe, α -nucleus potential for α -decay and sub-barrier fusion. *Phys. Rev. C* **72**, 064613 (2005). <https://doi.org/10.1103/PhysRevC.72.064613>
26. F. Niu, C.W. Ma, Z.Q. Feng et al., Effect of isospin diffusion on the production of neutron-rich nuclei in multinucleon transfer reactions. *Phys. Rev. C* **97**, 034609 (2018). <https://doi.org/10.1103/PhysRevC.97.034609>
27. Y.Z. Wang, J.P. Cui, Y.L. Zhang et al., Competition between α decay and proton radioactivity of neutron-deficient nuclei. *Phys. Rev. C* **95**, 014302 (2017). <https://doi.org/10.1103/PhysRevC.95.014302>
28. G. Gamow, Zur Quantentheorie des Atomkernes. *Z. Phys.* **51**, 204–212 (1928). <https://doi.org/10.1007/BF01343196>
29. R.W. Gurney, E.U. Condon, Wave mechanics and radioactive disintegration. *Nature* **122**, 3073 (1928). <https://doi.org/10.1038/122439a0>
30. Y.B. Qian, Z.Z. Ren, D.D. Ni, Z.Q. Sheng, Half-lives of proton emitters with a deformed density-dependent model. *Chin. Phys. Lett.* **27**, 112301 (2010). <https://doi.org/10.1088/0256-307X/27/11/112301>
31. J. Liu, Z. Wang, H.T. Zhang et al., Theoretical predictions on cluster radioactivity of superheavy nuclei with $Z=119, 120$. *Chin. Phys. C.* **48**, 014105 (2024). <https://doi.org/10.1088/1674-1137/ad0827>
32. X.D. Sun, P. Guo, X.H. Li, Systematic study of α decay half-lives for even-even nuclei within a two-potential approach. *Phys. Rev. C* **93**, 034316 (2016). <https://doi.org/10.1103/PhysRevC.93.034316>
33. H.F. Zhang, W. Zuo, J.Q. Li et al., α decay half-lives of new superheavy nuclei within a generalized liquid drop model. *Phys. Rev. C* **74**, 017304 (2006). <https://doi.org/10.1103/PhysRevC.74.017304>
34. X.J. Bao, H.F. Zhang, B.S. Hu et al., Half-lives of cluster radioactivity with a generalized liquid-drop model. *J. Phys. G Nucl. Part. Phys.* **39**, 095103 (2012). <https://doi.org/10.1088/0954-3899/39/9/095103>
35. J.P. Cui, Y.L. Zhang, S. Zhang et al., α -decay half-lives of superheavy nuclei. *Phys. Rev. C* **97**, 014316 (2018). <https://doi.org/10.1103/PhysRevC.97.014316>
36. C. Qi, F.R. Xu, R.J. Liotta, R. Wyss, Universal decay law in charged-particle emission and exotic cluster radioactivity. *Phys. Rev. Lett.* **103**, 072501 (2009). <https://doi.org/10.1103/PhysRevLett.103.072501>
37. S. Hofmann, G. Münzenberg et al., The discovery of the heaviest elements. *Rev. Mod. Phys.* **72**, 733 (2000). <https://doi.org/10.1103/RevModPhys.72.733>
38. Yu.T. Oganessian, Heaviest nuclei from ^{48}Ca -induced reactions. *J. Phys. G Nucl. Part. Phys.* **34**, 165–242 (2007). <https://doi.org/10.1088/0954-3899/34/4/R01>
39. S.H. Zhu, T.L. Zhao, X.J. Bao, Systematic study of the synthesis of heavy and superheavy nuclei in ^{48}Ca induced fusion evaporation reactions. *Nucl. Sci. Tech.* **35**, 124 (2024). <https://doi.org/10.1007/s41365-024-01483-5>
40. M.H. Zhang, Y.H. Zhang, F.S. Zhang et al., Possibilities for the synthesis of superheavy element $Z = 121$ in fusion reactions. *Nucl. Sci. Tech.* **35**, 95 (2024). <https://doi.org/10.1007/s41365-024-01452-y>
41. S. Madhu, H.C. Manjunatha, N. Sowmya et al., Cr induced fusion reactions to synthesize superheavy elements. *Nucl. Sci. Tech.* **35**, 90 (2024). <https://doi.org/10.1007/s41365-024-01449-7>
42. Yu.T. Oganessian, FSh. Abdullin, P.D. Bailey et al., Synthesis of a new element with atomic number $Z = 117$. *Phys. Rev. Lett.* **104**, 142502 (2010). <https://doi.org/10.1103/PhysRevLett.104.142502>
43. V.Y. Denisov, V.K. Utyonkov, FSh. Abdullin et al., Synthesis of the isotopes of elements 118 and 116 in the ^{249}Cf and $^{245}\text{Cm}+^{48}\text{Ca}$ fusion reactions. *Phys. Rev. C* **74**, 044602 (2006). <https://doi.org/10.1103/PhysRevC.74.044602>
44. V.Y. Denisov, V.K. Utyonkov, S.N. Dmitriev et al., Synthesis of elements 115 and 113 in the reaction ^{243}Am and ^{48}Ca . *Phys. Rev. C* **72**, 034611 (2005). <https://doi.org/10.1103/PhysRevC.72.034611>
45. V.Y. Denisov, V.K. Utyonkov, Yu.V. Lobanov et al., Experiments on the synthesis of element 115 in the reaction $^{243}\text{Am}(^{48}\text{Ca}, \text{xn})^{291-x}115$. *Phys. Rev. C* **69**, 021601 (2004). <https://doi.org/10.1103/PhysRevC.69.021601>
46. H.M. Liu, Y.T. Zou, X. Pan et al., Systematic study of the α decay preformation factors of the nuclei around the $Z = 82, N = 126$ shell closures within the generalized liquid drop model. *Chin. Phys. C.* **44**, 094106 (2020). <https://doi.org/10.1088/1674-1137/44/9/094106>
47. H.F. Zhang, G. Royer, α particle preformation in heavy nuclei and penetration probability. *Phys. Rev. C* **77**, 054318 (2008). <https://doi.org/10.1103/PhysRevC.77.054318>
48. S. Luo, D.M. Zhang, L.J. Qi et al., α particle preformation factor in heavy and superheavy nuclei. *Chin. Phys. C.* **48**, 044105 (2024). <https://doi.org/10.1088/1674-1137/ad21e9>
49. J. Dvorak, M. Chelnokov, P. Dressler et al., Doubly magic nucleus $^{270}_{108}\text{Hs}_{162}$. *Phys. Rev. Lett.* **97**, 242501 (2006). <https://doi.org/10.1103/PhysRevLett.97.242501>
50. J.G. Deng, H.F. Zhang, X.D. Sun, New behaviors of α -particle preformation factors near doubly magic ^{100}Sn . *Chin. Phys. C.* **46**, 061001 (2022). <https://doi.org/10.1088/1674-1137/ac5a9f>
51. S. Luo, L.J. Qi, D.M. Zhang et al., An improved empirical formula of α decay half-lives for superheavy nuclei. *Eur. Phys. J. A* **59**, 125 (2023). <https://doi.org/10.1140/epja/s10050-023-01040-5>
52. Y.Z. Wang, S.J. Wang, Z.Y. Hou et al., Systematic study of α -decay energies and half-lives of superheavy nuclei. *Phys. Rev. C* **92**, 064301 (2015). <https://doi.org/10.1103/PhysRevC.92.064301>
53. J.M. Dong, H.F. Zhang, J.Q. Li et al., Cluster preformation in heavy nuclei and radioactivity half-lives. *Eur. Phys. J. A* **41**, 197 (2009). <https://doi.org/10.1140/epja/i2009-10819-1>
54. Y.Z. Wang, J.Z. Cu, Z.Y. Hou, Preformation factor for α particles in isotopes near $N = Z$. *Phys. Rev. C* **89**, 047301 (2014). <https://doi.org/10.1103/PhysRevC.89.047301>
55. J.G. Deng, H.F. Zhang, Analytic formula for estimating the α -particle preformation factor. *Phys. Rev. C* **102**, 044314 (2020). <https://doi.org/10.1103/PhysRevC.102.044314>
56. C. Qi, D.S. Delion, R.J. Liotta, R. Wyss, Effects of formation properties in one-proton radioactivity. *Phys. Rev. C* **85**, 011303 (2012). <https://doi.org/10.1103/PhysRevC.85.011303>
57. Y.J. Wang, H.F. Zhang, W. Zuo et al., Improvement of a fission-like model for nuclear α decay. *Chin. Phys. Lett.* **27**, 062103 (2010). <https://doi.org/10.1088/0256-307X/27/6/062103>
58. Y.Z. Wang, F.Z. Xing, Jp. Cui et al., Roles of tensor force and pairing correlation in two-proton radioactivity of halo nuclei. *Chin. Phys. C* **47**, 084101 (2023). <https://doi.org/10.1088/1674-1137/acd680>
59. J.L. Chen, X.H. Li, X.J. Wu et al., Systematic study on proton radioactivity of spherical proton emitters within two-potential approach. *Eur. Phys. J. A* **57**, 305 (2021). <https://doi.org/10.1140/epja/s10050-021-00618-1>

60. T.K. Dong, Z. Ren, New model of binding energies of heavy nuclei with $Z \leq 90$. *Phys. Rev. C* **72**, 064331 (2005). <https://doi.org/10.1103/PhysRevC.72.064331>
61. G. Royer, Alpha emission and spontaneous fission through quasi-molecular shapes. *J. Phys. G Nucl. Part. Phys.* **26**, 1149 (2000). <https://doi.org/10.1088/0954-3899/26/8/305>
62. K.P. Santhosh, B. Priyanka, M.S. Unnikrishnan, Systematic study on alpha decay in $^{184-216}\text{Bi}$ nuclei. *AIP Conf. Proc.* **1524**, 135–138 (2013). <https://doi.org/10.1063/1.4801696>
63. K.P. Santhosh, Dashty T. Akrawy, Tinu Ann Jose et al., A systematic study of α -decay half-lives for Ac, Th, Pa, U and Np isotopes with $A = 205-245$ using the modified generalized liquid drop model. *Int. J. Mod. Phys. E* **32**, 2350047 (2023). <https://doi.org/10.1088/0954-3899/26/8/305>
64. N. Wang, M. Liu, X.Z. Wu et al., Surface diffuseness correction in global mass formula. *Phys. Lett. B* **734**, 215 (2014). <https://doi.org/10.1016/j.physletb.2014.05.049>
65. M.H. Zhang, Y.H. Zhang, F.S. Zhang et al., Progress in transport models of heavy-ion collisions for the synthesis of superheavy nuclei. *Nucl. Sci. Tech.* **46**, 080014 (2023). <https://doi.org/10.11889/j.0253-3219.2023.hjs.46.080014>
66. Z. Wang, Z. Ren, Predictions of the decay properties of the superheavy nuclei $^{293, 294}119$ and $^{294, 295}120$. *Nucl. Sci. Tech.* **46**, 080011 (2023). <https://doi.org/10.11889/j.0253-3219.2023.hjs.46.080011>
67. V.Yu. Denisov, A.A. Khudenko, α -Decay half-lives, α -capture, and α -nucleus potential. *Atom. Data Nucl. Data Tabl.* **95**, 815 (2009). <https://doi.org/10.1016/j.adt.2009.06.003>
68. F.G. Kondev, M. Wang, W.J. Huang et al., The NUBASE2020 evaluation of nuclear physics properties. *Chin. Phys. C* **45**, 030001 (2021). <https://doi.org/10.1088/1674-1137/abddae>
69. W.J. Huang, M. Wang, F.G. Kondev et al., The AME2020 atomic mass evaluation. *Chin. Phys. C* **45**, 030002 (2021). <https://doi.org/10.1088/1674-1137/abddb0>
70. M. Wang, W.J. Huang, F.G. Kondev et al., The AME2020 atomic mass evaluation. *Chin. Phys. C* **45**, 030003 (2021). <https://doi.org/10.1088/1674-1137/abddaf>
71. <https://www.nndc.bnl.gov>

Springer Nature or its licensor (e.g. a society or other partner) holds exclusive rights to this article under a publishing agreement with the author(s) or other rightsholder(s); author self-archiving of the accepted manuscript version of this article is solely governed by the terms of such publishing agreement and applicable law.